



HAL
open science

Thermal performance investigation of door opening and closing processes in a refrigerated truck equipped with different phase change materials

M.A. Ben Taher, Tarik Kousksou, Y. Zeraouli, M. Ahachad, M. Mahdaoui

► To cite this version:

M.A. Ben Taher, Tarik Kousksou, Y. Zeraouli, M. Ahachad, M. Mahdaoui. Thermal performance investigation of door opening and closing processes in a refrigerated truck equipped with different phase change materials. *Journal of Energy Storage*, 2021, 42, pp.103097. 10.1016/j.est.2021.103097 . hal-04482374

HAL Id: hal-04482374

<https://univ-pau.hal.science/hal-04482374>

Submitted on 22 Jul 2024

HAL is a multi-disciplinary open access archive for the deposit and dissemination of scientific research documents, whether they are published or not. The documents may come from teaching and research institutions in France or abroad, or from public or private research centers.

L'archive ouverte pluridisciplinaire **HAL**, est destinée au dépôt et à la diffusion de documents scientifiques de niveau recherche, publiés ou non, émanant des établissements d'enseignement et de recherche français ou étrangers, des laboratoires publics ou privés.



Distributed under a Creative Commons Attribution - NonCommercial 4.0 International License

1
2
3
4
5
6
7
8
9
10
11
12
13

Thermal performance investigation of door opening and closing processes in a refrigerated truck equipped with different phase change materials

M. A. Ben Taher ^{1,2*}, T. Kousksou ¹, Y. Zeraoui ¹, M. Ahachad ², M. Mahdaoui ²

¹ Université de Pau et des Pays de l'Adour (UPPA), Laboratoire des Sciences de l'Ingénieur Appliquées à la Mécanique et au Génie Electrique (SIAME), PAU, 64000, France

² Equipe de Recherche en Transferts Thermiques & Énergétique - Département de Physique FST, Université Abdelmalek Essaâdi Tanger, Morocco

Abstract

Refrigerated transport has been of interest to the scientific and industrial community for centuries. So far, temperature fluctuations during loading/unloading have been a major challenge. It is therefore essential to develop solutions to ensure the quality and safety of transported foodstuffs against temperature fluctuations as well as to reduce energy consumption and the environmental impact of commercial refrigerated trucks. The aim of the current work is to evaluate the aerothermal behavior of a refrigerated truck in two configurations (door open/closed) using different phase change materials throughout its operating cycle (charge and discharge). The results obtained show that the integration of a PCM in our system can significantly reduce the cooling capacity required when the truck door is opened and lead to significant energy savings by reducing greenhouse gas emissions.

25
26
27

Keywords: Energy storage, Emerging technologies, Refrigerated transport, Phase change materials, Food industry, CFD.

30

Nomenclature			
List of symbols		Acronyms	
h	convection coefficient ($\text{W m}^{-2} \text{K}^{-1}$)	CFD	computational fluid dynamic
Q	energy (J)	FR	filled ratio
g	gravitational acceleration (m s^{-2})	GHG	greenhouse gas
K	heat transfer coefficient ($\text{W m}^{-2} \text{K}^{-1}$)	MP	melting point
L_f	latent heat of fusion (kJ kg^{-1})	PCM	phase change material
C_p	specific heat capacity ($\text{J kg}^{-1} \text{K}^{-1}$)	RANS	reynolds averaged navier stokes
T	temperature (K)	RMSE	root mean square error
t	time (s)	SST	shear stress transport
I	turbulence intensity (%)		
k	turbulent kinetic energy ($\text{m}^2 \text{s}^{-2}$)		
u	velocity (m/s)		
v	volume (m^3)		
Subscripts			
c	curtain		
f	fluid		
g	goods		
l	liquid		
s	solid		
r	recovery		
w	wall		
Greek Letters			
η	efficiency (%)		
ρ	density (kg m^{-3})		
μ	dynamic viscosity (Pa s)		
λ	heat conductivity ($\text{W m}^{-1} \text{K}^{-1}$)		
μ_T	turbulent viscosity (Pa s)		
ε	turbulence dissipation rate ($\text{m}^2 \text{s}^{-3}$)		
σ	shear stress ($\text{kg m}^{-1} \text{s}^{-2}$)		
ω	specific turbulence dissipation rate (s^{-1})		

31

32 **1. Introduction**

33 Nowadays, as the world's population and economy steadily increasing, large amounts of
34 energy are consumed due to refrigeration equipment, leading to a wide variety of severe
35 energy and environmental impacts [1]. Moreover, this chain represents 30% of total world
36 energy consumption [2], and about 1% of global GHG emissions [3]. However, in most
37 instances where climate and energy policies are established, their major purpose is to reduce
38 dependence on fossil fuels and to meet the socio-economic needs of the population [4,5].
39 Furthermore, refrigerated transport has interested the scientific and industrial community for
40 centuries. Despite, the development of the cold chain does not meet all the requirements of the
41 standards applied in this sector.

42 Besides, refrigerated transport and storage of perishable foodstuffs will be more and more
43 required in the coming years [6]. Also, in the case of trucks, obtaining a constant air
44 temperature inside the trailer is more of a challenge than in buildings due to vehicle
45 movement [7]. Therefore, it is fundamental to contribute in cutting edge innovations for
46 refrigerated commercial trucks, to ensure the quality and the security of the products against
47 the temperature variations and to reduce the energy consumption and the environmental
48 impact during transport [8,9].

49 In this respect, scientists and engineers have been motivated to integrate thermal energy
50 storage (TES) based on phase change materials (PCM) in different sectors to enhance and to
51 improve the cold production system [10], including building cooling [11–14], solar absorption
52 refrigeration [15,16], industrial cooling [17–20] and cold storage applications [21–24].
53 Whereas the incorporation of a cold storage unit to conventional refrigeration systems could
54 reduce their cooling energy consumption by up to 50% [25].

55 Worldwide, an extensive effort has been made by various researchers on cold storage in
56 refrigerated trucks [26–33]. Tan et al. [30] shows the influence of heat transfer with
57 liquid/solid phase change in a truck using liquefied natural gas. The water as a PCM loaded
58 into the cold storage unit was solidified by the cryogenic natural gas. It was found that this
59 novel system significantly improves the internal thermal efficiency and phase change
60 performance. Ahmed et al. [31] discussed a new conventional method of reducing heat loss
61 for a refrigerated trailer. A decrease in heat transfer rate and total heat flux of 29.1% and
62 16.3%, respectively, was achieved when the different walls were incorporated with organic

63 PCMs. Consequently, these results contribute to a greater understanding of the importance of
64 these materials in reducing pollutant gases and extending the life of the cooling system.
65 Another design of the refrigerated truck incorporating PCM (melting point of $-26.7\text{ }^{\circ}\text{C}$) was
66 developed by Liu et al. [27] to maintain the required aerothermal conditions. The cooling
67 system charges the storage unit, during transport it provides internal cooling. The proposed
68 prototype shows energy savings of up to 86.4% and reduces GHG emissions compared to the
69 conventional system. Xia et al. [32] evaluated an insulated polystyrene container equipped
70 with PCM (MP= $-0.5\text{ }^{\circ}\text{C}$) to predict product temperature. The predictive model can be applied
71 in the industrial sector. Another study by Tinti et al. [34] on the application of PCM in
72 refrigerated transport, they studied the insulation of walls by integrating PCMs in
73 polyurethane foams. They concluded that a higher content of PCM in the foam results in
74 lower heat transfer in the hybrid insulation. Mousazade et al. [35] studied experimentally the
75 thermal performance of refrigerated truck by applying three types of PCMs in his cold
76 panels, they studied the effects of truck speed on the overall heat transfer coefficient and on
77 the temperature variations inside the box of the RT. Fioretti et al. [36] investigated the use of
78 PCMs in a refrigerator envelope via an experimental and theoretical study. By their developed
79 model, they estimated a reduction of 4.7% in the total energy required of the system.

80 For delivery trucks, the uniformity and the temperature variation during loading/unloading
81 represent major challenges. For this reason, the use of the phase change materials (PCMs) in
82 refrigerated trucks is a promising solution, as it guarantees product quality and protects the
83 cold chain. As a result, energy costs and environmental impact are reduced, improving energy
84 efficiency in the transport sectors. To the author's knowledge, the incorporation of a roof-
85 mounted tube bundle thermal energy storage unit of a refrigerated truck is an innovative
86 design. Namely, that the cooling system charges these rods, when the door is open the PCMs
87 provides the cold energy during its discharge. Following the validation of numerical model
88 with experimental results from the literature, the impetus for the current research is based on
89 the evaluation of aerothermal behavior using different PCMs, while increasing the thermal
90 mass of cooling system without significantly influencing the truck volume. Hence, this paper
91 aims at evaluating two configurations (opening/closing door) of conjugate and phase change
92 heat transfer by identifying the best PCMs during its complete cycle (charge and discharge).
93 Also, to evaluate the feasibility of the proposed concept for a temperature-controlled transport
94 in the range of $0\sim 12\text{ }^{\circ}\text{C}$. To this end, the energy savings and potential CO₂ reductions were
95 investigated for different scenarios in Europe. This paper is structured as follows. Section 2

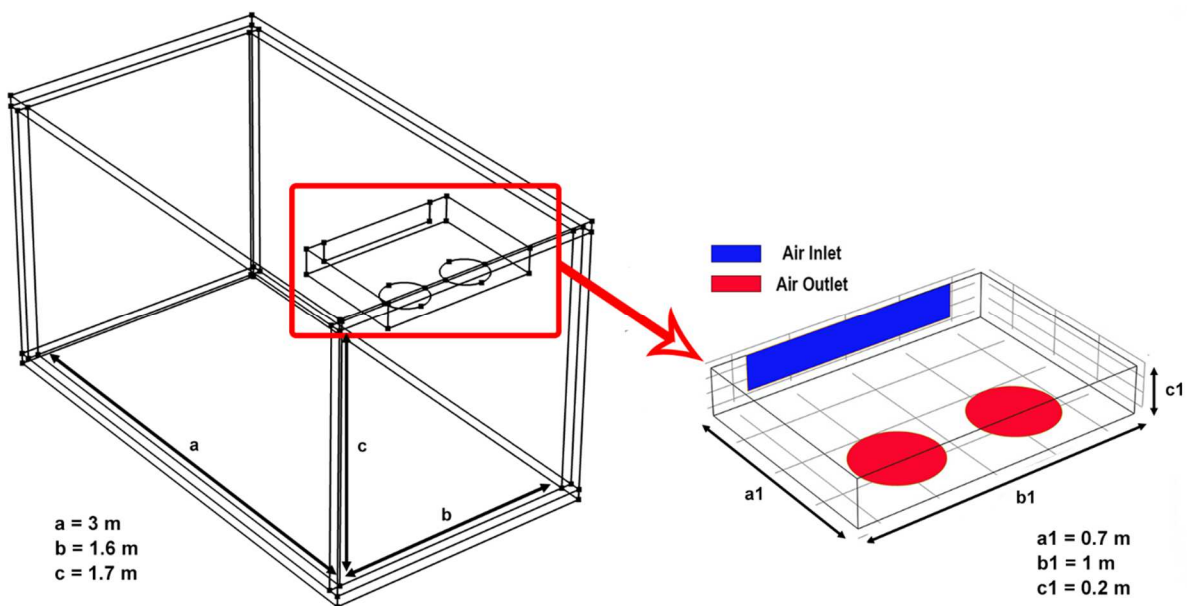
96 describes the system and the physical model. Section 3 provides the model validation. Section
97 4 discusses the results. The last section deals with the study's conclusion.

98 2. System description and methodology

99 This work deals with two configurations of a refrigerated truck, one with a closed-door
100 already studied experimentally [Fig. 1], and the other design with an open door was then
101 investigated. Both designs have the same geometry and their internal dimensions were ~ 1.6
102 m wide, ~ 1.7 m long and ~ 3 m deep [Fig. 2]. A polyurethane foam insulation is
103 implemented in the walls, its thickness is 0.1 m for the floor and 0.07 m for the remaining
104 walls. The thermal properties of the polyurethane are determined at 50 (kg m^{-3}), 1470 (J kg^{-1}
105 K^{-1}), and 0.022 ($\text{W m}^{-1} \text{K}^{-1}$) for density, specific heat capacity, and thermal conductivity,
106 respectively [37].

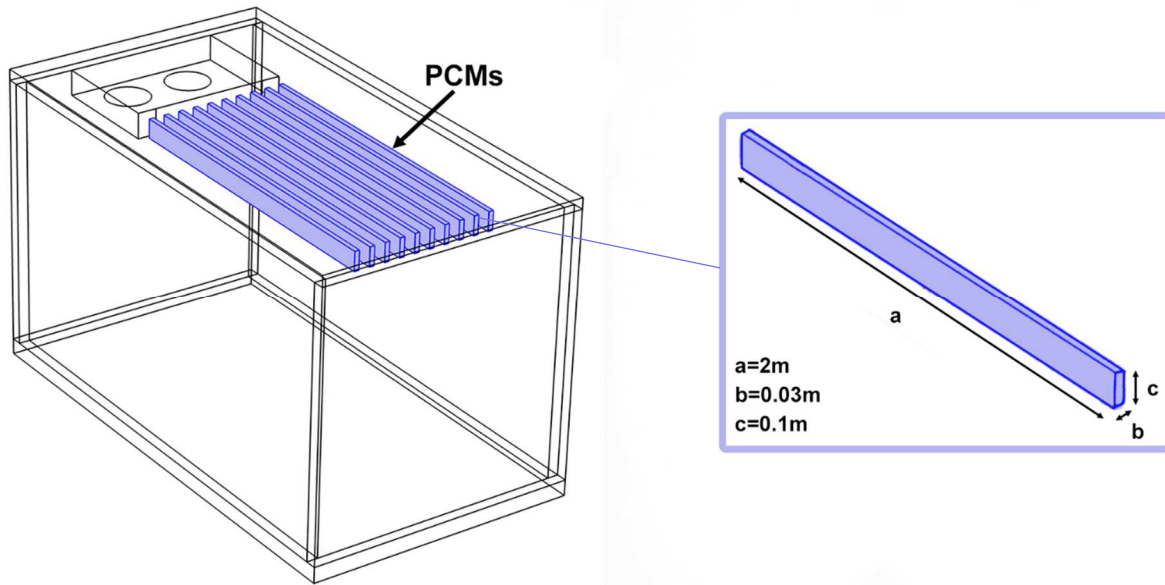


107
108 **Fig.1** Real delivery refrigerated truck [38]
109



112 **Fig.2** 3D-CFD models of empty truck geometry

113 To minimize air temperature fluctuations during the loading or unloading period, some
 114 parallelepiped rods confining a PCM have been installed and fixed on the ceiling of the
 115 refrigeration compartment [**Fig. 3**]. As aluminum provides lighter structures while
 116 maintaining a high thermal conductivity to intensify the charge-discharge process of the
 117 contained PCM. For this reason, it is assumed that the baffle-type panels are constructed of
 118 aluminum, with a thin thickness of 2 mm. Besides, a space was also maintained between the
 119 rods to permit air circulation and to improve the contact between the cold air and the PCM.



120
 121 **Fig.3** 3D truck geometry model with PCMs incorporated.

122 Obviously, the main requirement for PCMs selection were a suitable melting temperature
 123 range with the cooling system and a specific heat capacity above 150 kJ/kg [39]. Moreover,
 124 **Table 1** lists the principal thermophysical properties of different PCMs that were examined.
 125 The objective of this study is to store the cold in the PCM during the charging process and
 126 recuperate it during the discharging phase to mitigate the impact of opening the doors.

127 **Table 1** Thermo-physical characteristics of PCMs [40]

Characteristics	Units	RT3 HC1	RT5	RT8 HC
Density liquid ρ_l	kg m ⁻³	770	770	770
Density solid ρ_s	kg m ⁻³	880	880	880
Phase change temperature T_f	°C	3	5	8
Transition interval temperature $\Delta T_{l \leftrightarrow s}$	°C	2	2	2
Flash point	°C	110	113	120
Latent heat of fusion L_f	kJ kg ⁻¹	190	180	190

Heat conductivity (both phases) $\lambda_{s,l}$	W m ⁻¹ K ⁻¹	0.2	0.2	0.2
Specific heat capacity Cp	J kg ⁻¹ K ⁻¹	2000	2000	2000

128 3. Mathematical modelling

129 3.1. Model assumptions

130 To simplify our study and to establish the energy balances in our system, the following
131 assumptions are used:

- 132 • The air is Newtonian and incompressible.
- 133 • The air flow is turbulent and viscous
- 134 • The thermophysical properties of air are temperature dependent.
- 135 • The Boussinesq approximation and the gravity effect are considered.
- 136 • The PCM exhibit an isotropic and homogeneous structure.
- 137 • The phase change process (melting/crystallization) occurs over a small range of
138 temperature.
- 139 • The heat transfer across the PCM packaging thickness is neglected.
- 140 • The natural convection effect during the phase change process is neglected.

141

142 3.2. Governing equations

143 In this work, two types of operation have been analyzed for the truck, the first one consists
144 essentially in a forced turbulent refrigeration process provided by the refrigeration unit, while
145 for the second one, a natural convection takes place when the doors of the truck are open.

146 3.2.1. For air inside the closed-door truck

147 To describe the air-flow and heat transfer in the refrigerated chamber, Eqs. (1) - (4) are used.
148 In addition, to evaluate the aerothermal performance inside the refrigerated truck during the
149 closed-door operation, three turbulence models are tested and compared: standard k- ω SST
150 Eq. (5) and (6) [41], standard k- ω Eq. (7) and (8) [42] and k- ϵ Eq. (9) and (10) [43].

$$\frac{\partial \rho_f}{\partial t} + \nabla \cdot (\rho_f u_f) = 0 \quad (1)$$

$$\rho_f \frac{\partial u_f}{\partial t} + \rho_f (u_f \cdot \nabla) u_f = \nabla \cdot [-pI + K] - \frac{2}{3} (\mu_f + \mu_T) (\nabla \cdot u_f) I - \frac{2}{3} \rho_f k I + (\rho_f - \rho_{f,0}) \vec{g} \quad (2)$$

$$K = (\mu_f + \mu_T) (\nabla u_f + (\nabla u_f)^T) \quad (3)$$

$$\rho_f C_{p,f} \frac{\partial T_f}{\partial t} + \nabla \cdot (\rho_f C_{p,f} u_f T_f - k \vec{\nabla} T_f) = 0 \quad (4)$$

* k – ω SST model

$$\rho_f \frac{\partial k}{\partial t} + \rho_f (u_f \cdot \nabla) k = \nabla \cdot [(\mu_f + \mu_T \sigma_k^*) \nabla k] + P_k - \rho_f \beta_0^* k \omega \quad (5)$$

$$\begin{aligned} \rho_f \frac{\partial \omega}{\partial t} + \rho_f (u_f \cdot \nabla) \omega \\ = \nabla \cdot [(\mu_f + \mu_T \sigma_\omega) \nabla \omega] + \frac{\gamma}{\mu_T} \rho_f P_{SST} - \rho_f \beta_0 \omega^2 + 2(1 - f_{v1}) \frac{\sigma_{\omega 2} \rho_f}{\omega} \nabla k \cdot \nabla \omega \end{aligned} \quad (6)$$

* k – ω model

$$\rho_f \frac{\partial k}{\partial t} + \rho_f (u_f \cdot \nabla) k = \nabla \cdot [(\mu_f + \mu_T \sigma_k^*) \nabla k] + P_k - \rho_f \beta_0^* k \omega \quad (7)$$

$$\rho_f \frac{\partial \omega}{\partial t} + \rho_f (u_f \cdot \nabla) \omega = \nabla \cdot [(\mu_f + \mu_T \sigma_\omega) \nabla \omega] + \alpha \frac{\omega}{k} P_k - \rho_f \beta_0 \omega^2 \quad (8)$$

* Standard k – ε model

$$\rho_f \frac{\partial k}{\partial t} + \rho_f (u_f \cdot \nabla) k = \nabla \cdot \left[\left(\mu_f + \frac{\mu_T}{\sigma_k} \right) \nabla k \right] + P_k - \rho \varepsilon \quad (9)$$

$$\rho_f \frac{\partial \varepsilon}{\partial t} + \rho_f (u_f \cdot \nabla) \varepsilon = \nabla \cdot \left[\left(\mu_f + \frac{\mu_T}{\sigma_\varepsilon} \right) \nabla \varepsilon \right] + C_{\varepsilon 1} \frac{\varepsilon}{k} P_k - C_{\varepsilon 2} \rho_f \frac{\varepsilon^2}{k} \quad (10)$$

151 where T_f, u_f, ρ_f, μ_f are the temperature, velocity, density, viscosity of air, respectively, k is
 152 the turbulent kinetic, μ_T is the turbulent viscosity $\mu_T = \rho k / \omega$, ω is the turbulent dissipation
 153 rate, ε is the turbulent kinetic energy rate, I is the turbulence intensity, and $\beta_0, \beta_0^*, \sigma_k,$
 154 $\sigma_\omega, P_k, C_\varepsilon$ are the adjustable turbulence parameters for the different models.

155 3.2.2. For air inside the opened-door truck

156 Further, the cooling unit turned off when the door was opened. The difference in air
 157 temperature (between outside and inside) induces a natural convection in the chamber. The
 158 airflow and heat transfer inside the truck in this case are governed by the following equations
 159 Eqs. (11) - (14).

$$\rho_f \frac{\partial u_f}{\partial t} + \rho_f (u_f \cdot \nabla) u_f = \nabla \cdot [-pI + K_{op}] + (\rho_f - \rho_{f,0}) \vec{g} \quad (11)$$

$$\frac{\partial \rho_f}{\partial t} + \nabla \cdot (\rho_f u_f) = 0 \quad (12)$$

$$K_{op} = \mu_f \left(\nabla u_f + (\nabla u_f)^{T_f} \right) - \frac{2}{3} \mu_f (\nabla \cdot u_f) I \quad (13)$$

$$\rho_f C_{p,f} \frac{\partial T_f}{\partial t} + \nabla \cdot (\rho_f C_{p,f} u_f T_f - k \vec{\nabla} T_f) = 0 \quad (14)$$

160

161 3.2.3. For the chamber walls

162 The heat transfer in all walls is described by Eq. (15):

$$\rho_w C_{p,w} \frac{\partial T_w}{\partial t} + \nabla \cdot (\lambda_w \vec{\nabla} T_w) = 0 \quad (15)$$

163 where $T_w, \rho_w, C_{p,w}, \lambda_w$ are the temperature, density, specific heat, and conductivity of the
164 wall.

165

166 3.2.4. For PCMs

167 To describe the heat transfer inside the PCM, the enthalpy method has been applied which is
168 based on the following Eqs. (16) - (20) [44,45].

$$\frac{\partial(\rho_{pcm}H)}{\partial t} = \nabla \cdot (\lambda_{pcm} \nabla T_{pcm}) \quad (16)$$

169 Therefore, the specific enthalpy (H) is defined by the sum of both sensible and the latent heat.

$$H = h + \Delta H \quad (17)$$

$$h = h_{ref} + \int_{T_{ref}}^T C_{p,pcm} dT \quad (18)$$

$$\Delta H = fL \quad (19)$$

170 Equation 20 is used to evaluate the liquid fraction (f) at each cell:

$$f = \begin{cases} 1, & \text{if } T_{pcm} > T_L \\ 0, & \text{if } T_{pcm} < T_S \\ \frac{T_{pcm} - T_S}{T_L - T_S}, & \text{if } T_L < T_{pcm} < T_S \end{cases} \quad (20)$$

171 where T_L is the liquidus temperature, T_S is the solidus temperature, $T_{pcm}, \rho_{pcm}, \lambda_{pcm}, C_{p,pcm}$
172 the temperature, density, heat capacity, and the conductivity of the PCM, respectively, and L
173 is the latent heat of the PCM.

174

175

176

177

178 **3.2.5. Energy efficiency**

179 The recovery energy (Q_r) and the energy efficiency (η) with PCMs were determined based on
180 the approaches Eq. (21) and (22), respectively.

$$Q_r = \int_{v_f} \rho_f C_{p,f} (T_f - T_0) dv_f \quad (21)$$

$$\eta = 1 - \frac{Q_r}{Q_{r0}} \quad (22)$$

181 where Q_{r0} the recovery energy through the open door, without incorporating PCM.

182 **3.3. Initial and boundary Conditions**

183 The previous equations are initiated by the following conditions:

- 184 - The ventilation conditions of cooling unit with the door closed case (forced convection)
185 were defined by a mean inlet velocity of $U_{0y}=U_0=3$ m/s.
- 186 - The temperature employed to blow air into the truck (inlet condition) was considered as
187 a correlation fitted from the experimental data Eq. (23) [38].

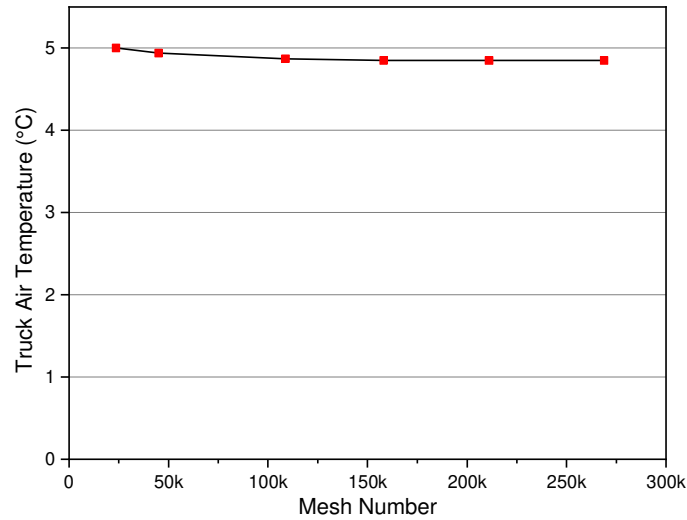
$$T_f(t) = 11.95 \exp(-0.001058 t) + 11.58 \exp(0.01036 t) \quad (23)$$

- 188 - The convection coefficient through the external face of walls was assumed to be:
189 $h_e=3.41$ W m⁻² K⁻¹
- 190 - When the cooling unit switched off, the heat transfer applied in the opened door case
191 (natural convection) is governed by the following equation Eq. (24):

$$\begin{aligned} T_f &= T_{ext} \text{ if } u_f < 0 \text{ (} T_{ext}: \text{ External temperature)} \\ -\lambda_f \nabla T_f &= 0 \text{ if } u_f \geq 0 \text{ (Zero heat flux condition)} \end{aligned} \quad (24)$$

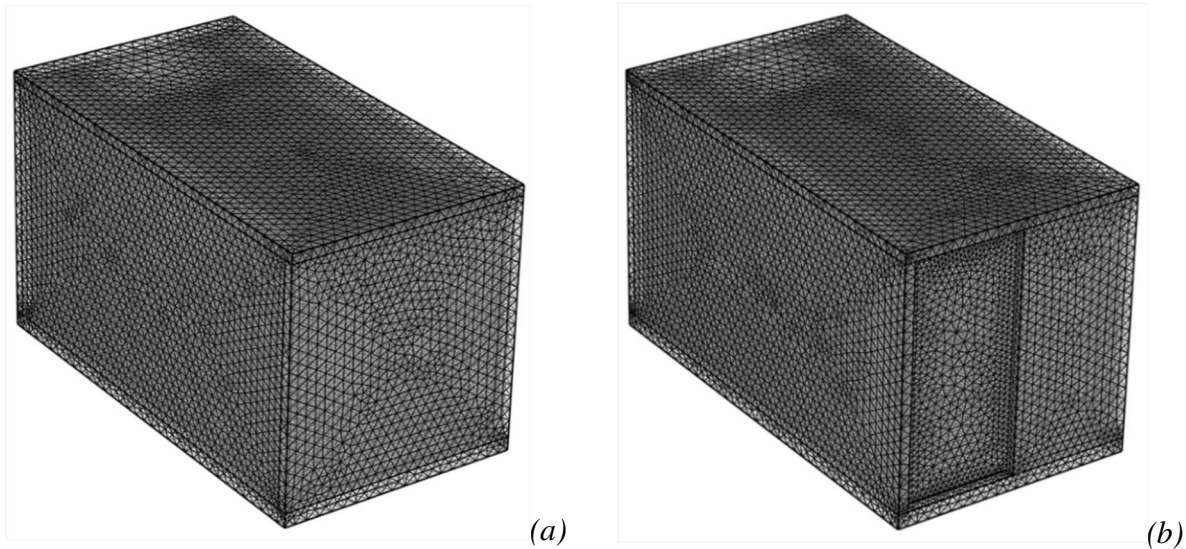
192 In this paper, the numerical model was implemented in COMSOL Multiphysics to simulate
193 the fluid dynamics and the conjugate heat transfer inside the refrigerated truck.

194 A sensitivity study on the effect of the mesh density on the obtained results was performed
195 [see Fig.4]. A mesh size of ≈ 150713 and ≈ 158033 with triangular elements was selected
196 for opened and closed truck's door geometry [Fig.5 (a) (b)], which gives satisfactory results
197 for both configurations. The time interval 10^{-3} s is chosen as it provides an accurate result.



198
199

Fig.4. Mesh independence test for closed door truck geometry



200

Fig. 5 Mesh defined in the geometry of (a) closed (b) open door truck geometry

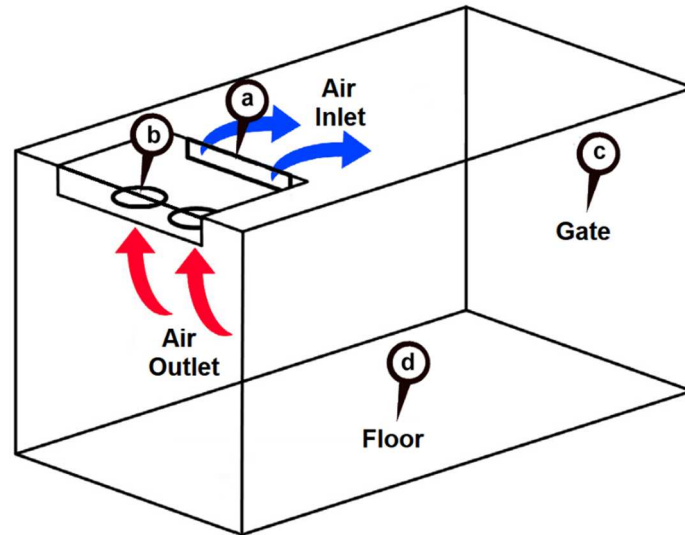
201 4. Result and analysis

202 4.1. Model validation

203 The first part of this study aims to validate the aerothermal behavior with different models of
 204 URANS unsteady turbulence (standard $\kappa\text{-}\omega$, SST $\kappa\text{-}\omega$, standard $\kappa\text{-}\epsilon$). During this phase, the air
 205 temperature inside the closed door refrigerated truck decreases due to the cooling system.
 206 Once the air temperature reaches the programmed set value, the cooling system is turned off.
 207 Comparisons were made between experimental temperature from literature [38] and the
 208 present numerical study at different locations (Inlet, Outlet, Gate and Floor) of the refrigerated
 209 compartment [Fig. 6]. The experimental data were collected by DS18B20 temperature sensors
 210 with an accuracy up to $\pm 0.5^\circ\text{C}$. These sensors were installed at different locations in a

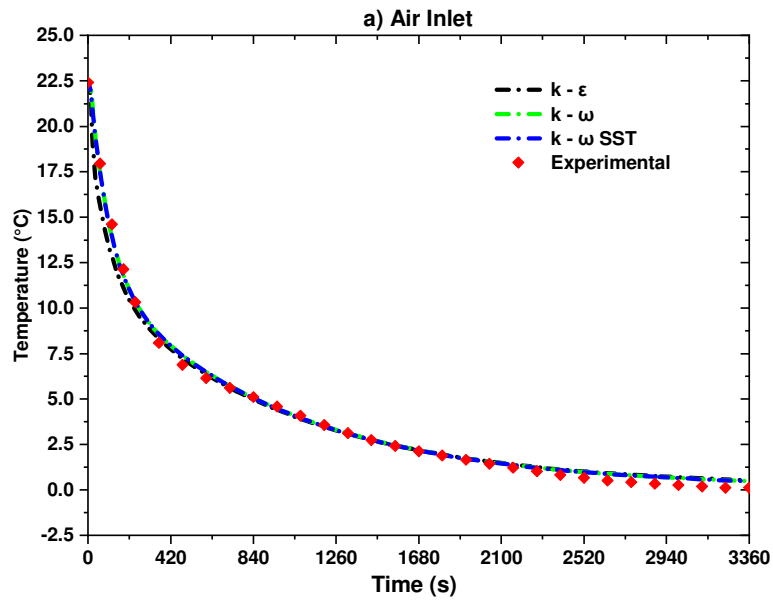
211 refrigerated compartment (four sensors for each selected location [Fig. 2]). Further, a
212 LUTRON digital anemometer was used to measure the mid-flow velocity through the
213 evaporator.

214 Comparing the measured and simulated values of the air temperatures inside the truck, it is
215 clearly that the numerical results show comparable values to data based on experimental
216 measurements [Fig. 7]. Therefore, the results of this study clearly demonstrate the ability of
217 URANS turbulence models to accurately predict experimental results. As well, to enhance the
218 validity of this work, the root mean square error (RMSE) values for the three turbulent models
219 were described and compared [Table. 2]. However, since the k- ω SST model combines both
220 models (k- ω and k- ϵ) which allows it to accurately assess the areas near and far from the
221 walls. It is clear that the RMSE values obtained with this model showed better agreement,
222 justifying the choice of this model in the rest of our work.

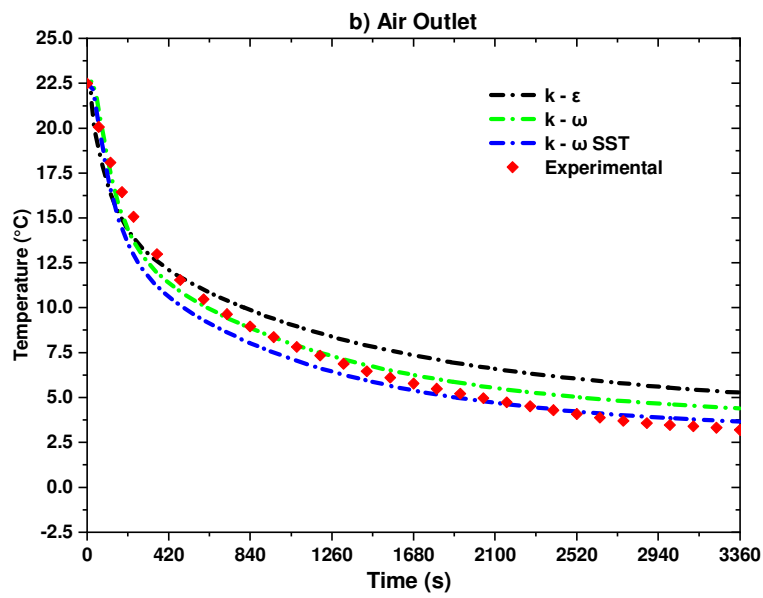


223
224

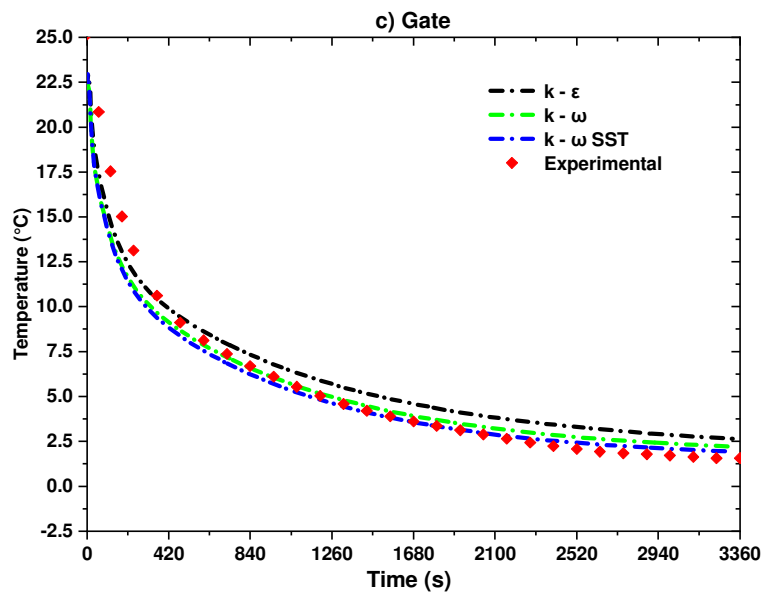
Fig. 6 Refrigerated compartment analysis locations



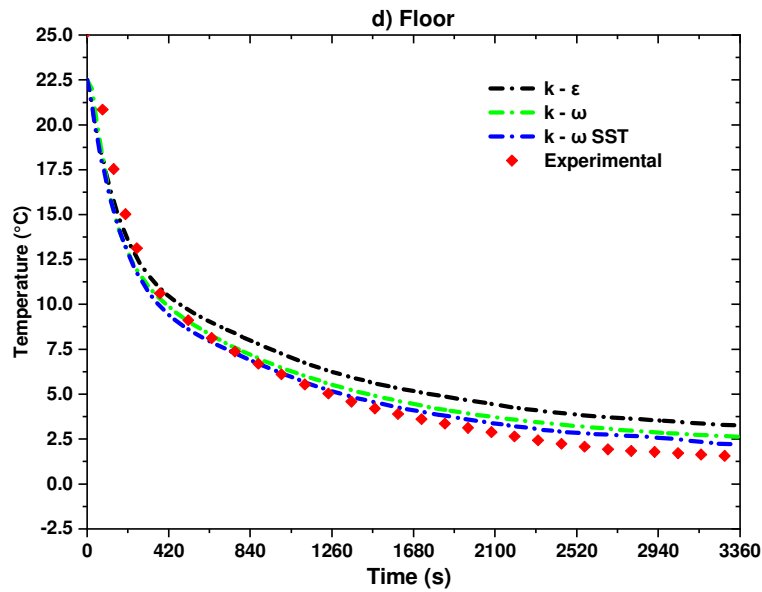
225



226



227



228
229

Fig. 7 Temperature values in different zones of the refrigerated truck

230 **Table 2** RMSE values for three simulated models in the different points of analysis

	RMSE k-ω-SST	RMSE k-ω	RMSE k-ε
Inlet	0,286 °C	0,299 °C	0,492 °C
Outlet	0,798 °C	0,804 °C	1,517 °C
Floor	0,914 °C	1,071 °C	1,586 °C
Gate	1,222 °C	1,224 °C	1,283 °C
Global	0,805 °C	0,849 °C	1,219 °C

231

232 4.2. Closed/open truck performance

233 Once the model is validated, the energy performance of the closed/open truck through a
 234 suggested scenario in this work. The CFD SST k-omega model was used in the rest of this
 235 work after verifying its ability to accurately describe the aerothermal behavior through the
 236 truck. This scenario is based on several cycles, each entire cooling cycle (cooling system
 237 switch on and off) assuming that the door closing phase has an estimated trip time of 60 min
 238 with an initial truck temperature of 22.5°C [Fig.8].



239

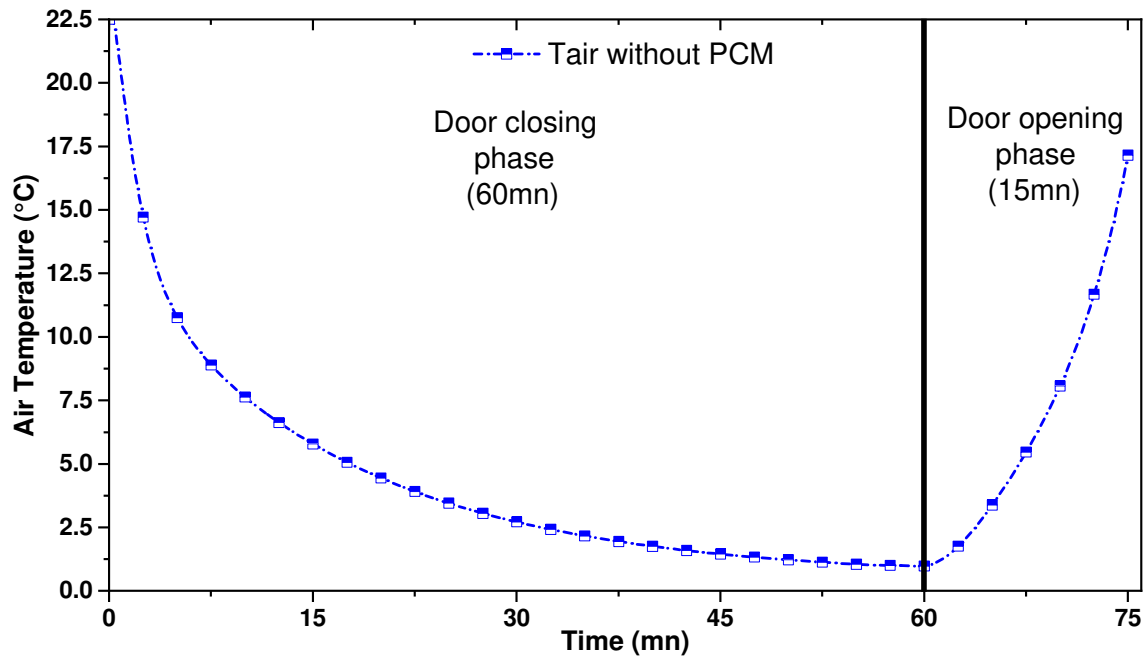
240

Fig.8 Proposed truck itinerary during cooling system on/off cycles

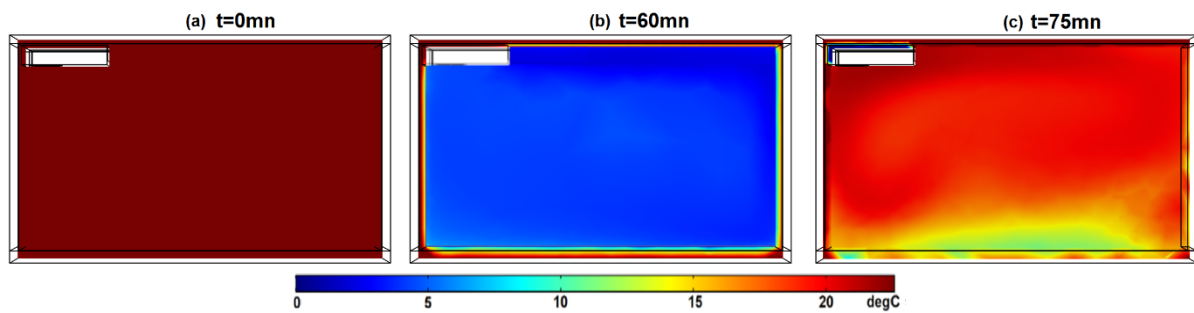
241 To understand the aerothermal behavior of the closed- and open-door truck, the following
 242 **[Fig.9]** represents the temperature distribution during one cycle at different times of truck
 243 without PCM for both phases. At initial instant, the temperature was about 22°C **[Fig.10.a]**.
 244 During the cooling period (door closed / truck on the road), the coldest area is located at the
 245 roof, while it increases in the rest of truck. The cooling process continues until the desired
 246 temperature is reached almost uniformly in all areas of the truck **[Fig.10.b]**.

247 Then during the second scenario, which lasts 15 minutes, the cooling system is stopped and
 248 the door is opened. In this case, the hot air enters the truck and creates a natural convection
 249 phenomenon that leads to an increase of the air temperature in the truck. The hot air flows
 250 upwards and the cold air flows downwards **[Fig.10.c]**.

251



252
253 **Fig.9** Evolution of the air temperature inside the truck during cooling system on/off cycle



254
255 **Fig.10** Temperature profile patterns during cooling system on/off cycle for various instants.

256 **4.3. Influence of PCM incorporation**

257 Basically, the truck door must remain open during loading or unloading. However, air
258 infiltration during these periods increases considerably the cooling energy consumption. For
259 this reason, the use of PCMs in refrigerated trucks could present a promising solution that
260 allows cold storage during the operation of the cooling system and improves the performance
261 of the truck, resulting in energy savings.

262 For this purpose, a baffle-type PCM panels were confined in a roof-mounted unit [Fig.3].
263 Three PCMs were chosen (RT3 HC1, RT5 and RT8 HC) according to their melting
264 temperature (3 °C, 5 °C and 8 °C) and tested during a complete cycle (on and off).

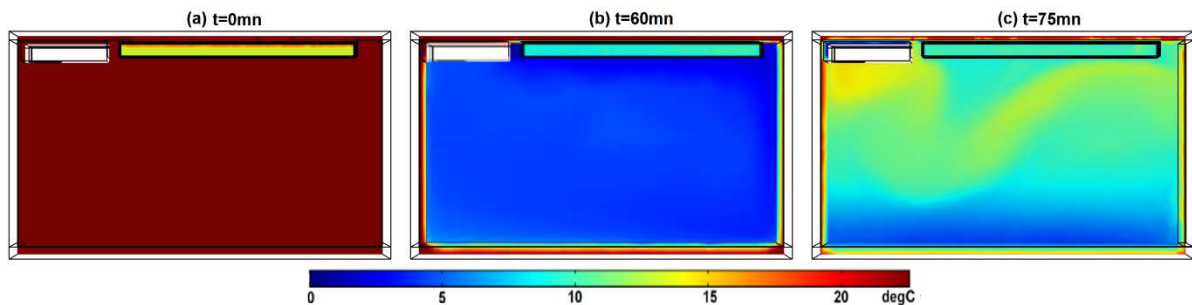
265 The results of the different tests have been classified into the following scenarios:

- 266 1. Cycles in which the PCM is completely melted as an initial phase, the latter is
267 charged by the refrigeration system during transport.

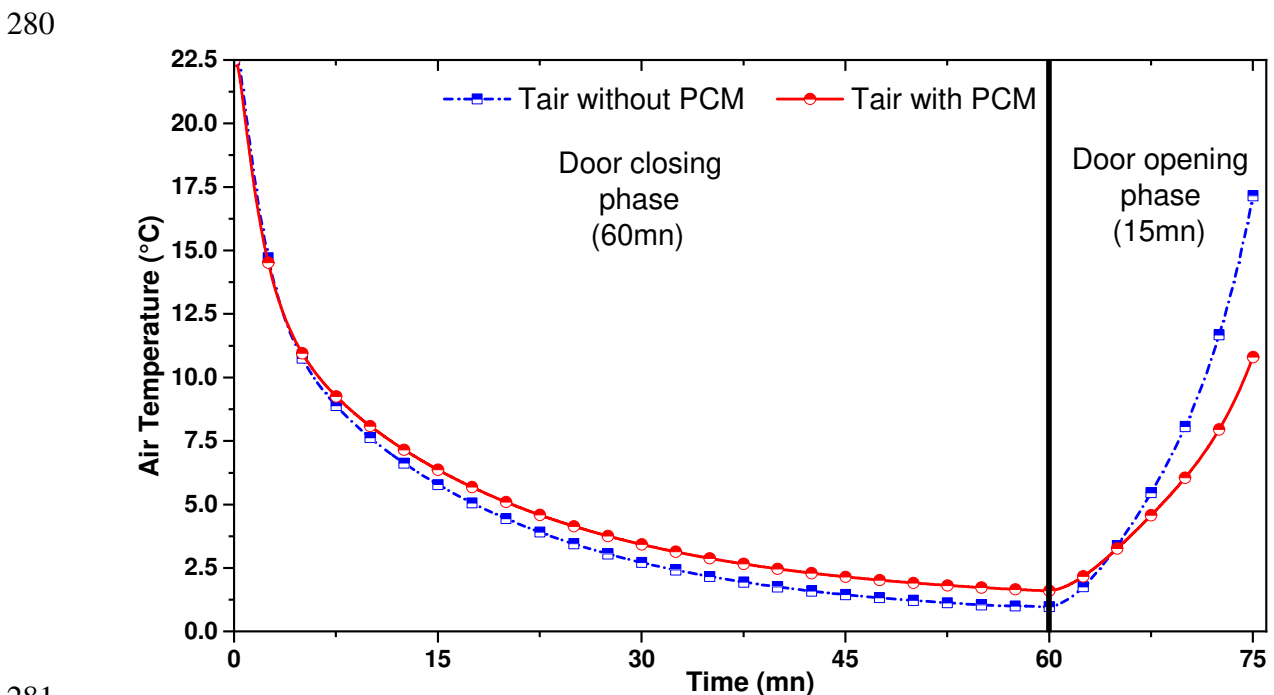
268 2. Cycles in which the PCM cannot freeze completely due to the cooling system
269 turning off (frequent door openings).

270 At first, a detailed analysis was made to evaluate the impact of RT8 HC PCM on the truck's
271 performance. [Fig.11] presents the median plane of the temperature distribution during one
272 cycle incorporating RT8 HC PCM. As can be noticed, during the closed-door period, PCM
273 begins to be charged through the enabled cooling system.

274 Besides, as can be seen [Fig. 12], due to the latent heat of the PCM, there is small difference
275 in the truck's internal temperatures during cooling when comparing the results without PCM
276 for the first cycle. Moreover, the air leakage is significantly reduced compared to the model
277 without PCM during the open phase.



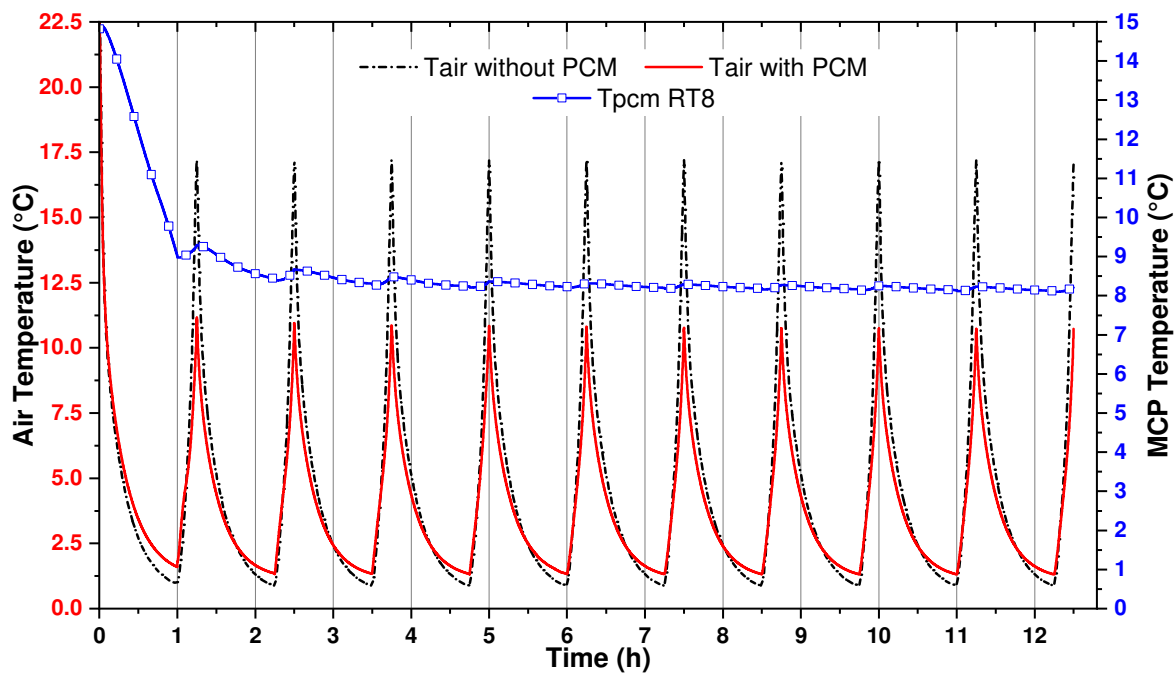
278
279 **Fig.11** Evolution of the air temperature inside the truck with PCM during cooling cycle



281
282 **Fig.12** Evolution of the air temperature inside the truck with PCM during cooling cycle

283 To fully understand PCMs' effect, [Fig. 13] shows the average air temperature with and
 284 without PCMs during ten studied cycles (door closures (openings) of 60 min (15 min) in each
 285 cycle), and the PCM temperature distributions at the beginning and end of the process. As
 286 expected, the benefit of the PCM (RT8 HC) inside the truck is evident to maintain and reduce
 287 temperature fluctuations when opening the doors. Moreover, to ensure the safety of perishable
 288 foodstuffs, a maximum temperature of 12 ° C is required in the refrigeration compartment
 289 [46,47].

290 Once the cooling system is turned on, the average temperature decreases from about 20 to 1°C
 291 and from 20 to 2°C during 60 min for the configuration without and with PCM, respectively.
 292 The effect of PCM integration is negligible within the first cycle, as it has not yet reached its
 293 phase change. When the door is open, the average temperature increases from about 1 to 17°C
 294 and 2 to 11°C during 15 min for the configuration without and with PCM, respectively.
 295 Hence, thermal performance has been significantly improved when incorporating PCM. In the
 296 following cycles, the benefits of PCM are obvious. Thus, the upper-temperature limit is
 297 already exceeded for the reference configuration, and the internal temperature of the container
 298 was maintained in the range of 2-11 ° C using RT8 HC as PCM. However, the results also
 299 show that the addition of the PCM at the highest airflow area leads to faster energy storage at
 300 the beginning of the charging process. Also, the melting/solidification cycle is mainly driven
 301 by the number of start-ups and shutdowns of the refrigeration system.



302

303

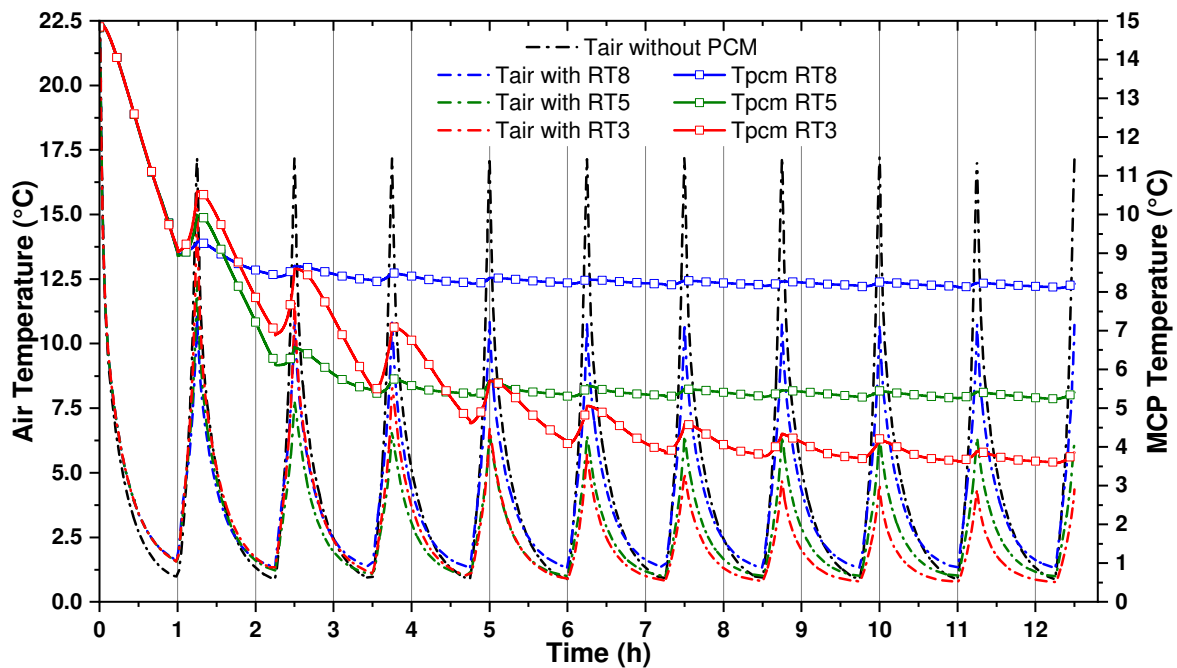
Fig. 13 Average air temperature (a) without and (a) with RT8 HC PCM

304

305 4.4. Comparison between the incorporation of several PCMs

306 Furthermore, the performances of different PCMs (RT3 HC1, RT5, RT8 HC) are compared
307 into the reference case (without PCM) to identify the best configuration that guarantees the
308 desired temperature range [Fig. 14]. Among the three configurations presented, the
309 configuration with **RT5** has maintained a maximum temperature of $\sim 6^\circ\text{C}$ as soon as the
310 fourth cycle is reached ($\sim 4\text{h}$). This shows that a medium-distance refrigerated transport with
311 this configuration is preferable and it would be able to maintain perishable products during
312 this period such as industrial milk, butter, and meat products.

313 As a result, the use of PCM-RT3 HC1 offers better aerothermal transfer performance to reach
314 the stabilization temperature inside the truck of $\sim 4^\circ\text{C}$. This configuration would be ideal for
315 highly perishable foodstuffs with special requirements such as milk (raw or pasteurized) for
316 consumption, dairy products (kefir, cream, fresh cheese, and yogurt), egg products, and
317 poultry meats.



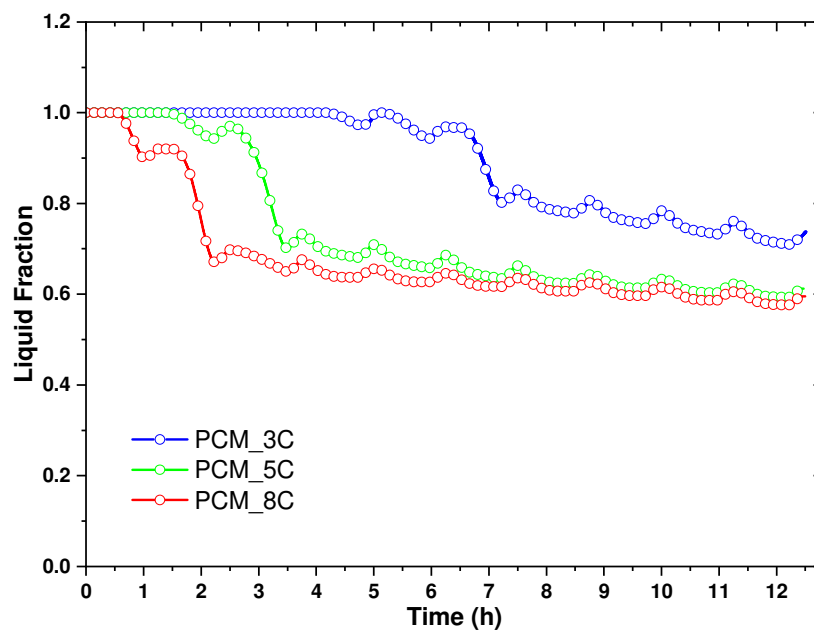
318

319 **Fig.14** Average air temperature (a) without and (a) with different PCMs

320 [Fig.15] illustrates the liquid fraction as a function of time (ten cycles) for the three PCMs. In
321 all three cases, the PCM partially solidifies/melts during its charge/discharge. This is due to
322 the temperature fluctuation when opening and closing the truck door for each cycle. It is also

323 noted that the liquid fraction values for PCM had the highest melting point (RT8 HC) is
324 always lower than the other PCMSs (RT5, RT3 HC1).

325 Moreover, the use of PCM could be an interesting alternative to maintain temperature
326 fluctuations in refrigerated trucks during periods after turning off the cooling system. Besides,
327 it is also interesting to note that the thermal mass inside the containers increases without
328 significantly increasing its volume, which could lead to more stable operation, longer
329 refrigeration system life, energy savings, and a decrease in GHG gases.



330

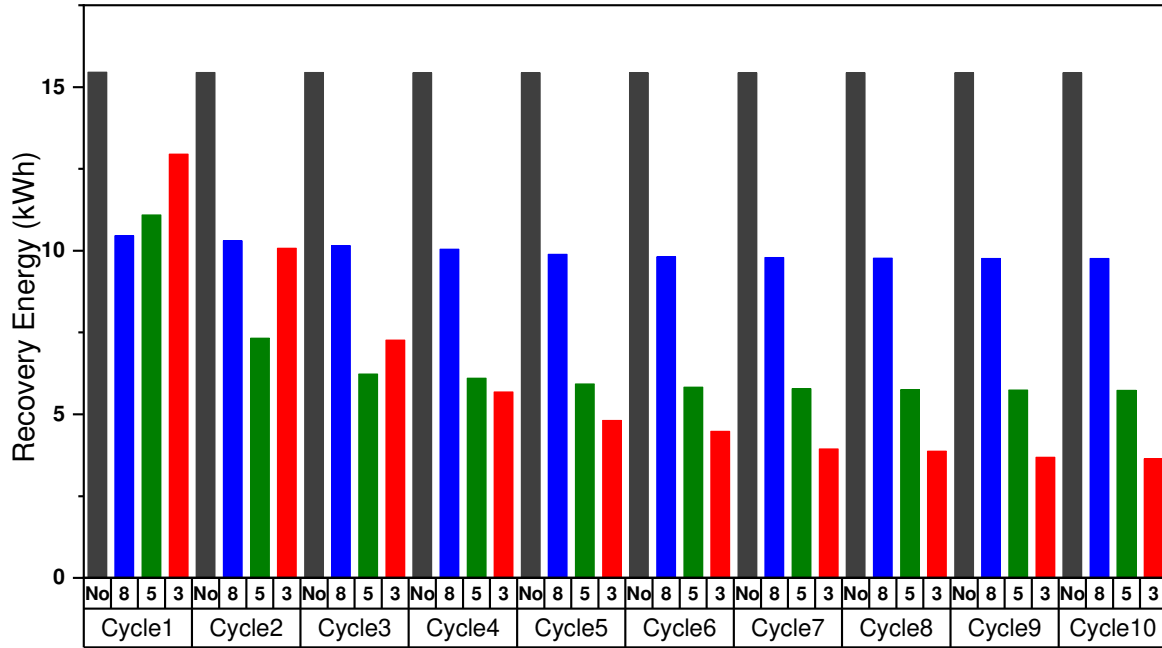
331

Fig.15 Variation of liquid fraction for different PCMs

332 4.5. Recovery cooling capacity

333 [Fig. 16] shows the recovery energies for a 15-minute door opening time during the test
334 periods. Cold storage capacity performance was evaluated for the reference container and
335 compared with the different PCM concepts (RT3 HC1, RT5, and RT8 HC). During each
336 cycle, hot air infiltration occurs during all periods, which leads to an increase in the recovery
337 energy. Table 3 shows that their average values are 57.62 kJ for the reference case and 36.94
338 kJ, 24.27 kJ and 22.38 kJ when using RT3 HC1, RT5 and RT8 HC, respectively. These values
339 are important as they represent the amount of energy that must be supplied by the
340 refrigeration system to re-cool the truck. Note that the energy balance does not include the
341 technical maintenance aspects of the storage system.

342 In general, temperatures in the truck with PCMs were lower than the reference truck without
 343 PCM due to the heat storage effect. Therefore, the recovery energy through the compartment
 344 is reduced when using PCM, which promotes the efficiency of incorporating a storage system.
 345 Furthermore, it is also worth noting that the high recovery energy corresponds to cycles with a
 346 partially melted PCM, and hence a lower improvement. For this reason, the energy values are
 347 higher for the concept with RT8 HC compared to other configurations.



348 **Fig. 16** Recovery energy of internal air without and with PCMs

349

350 **Table 3** Total recovery cooling capacity and energy saving without and with PCMs

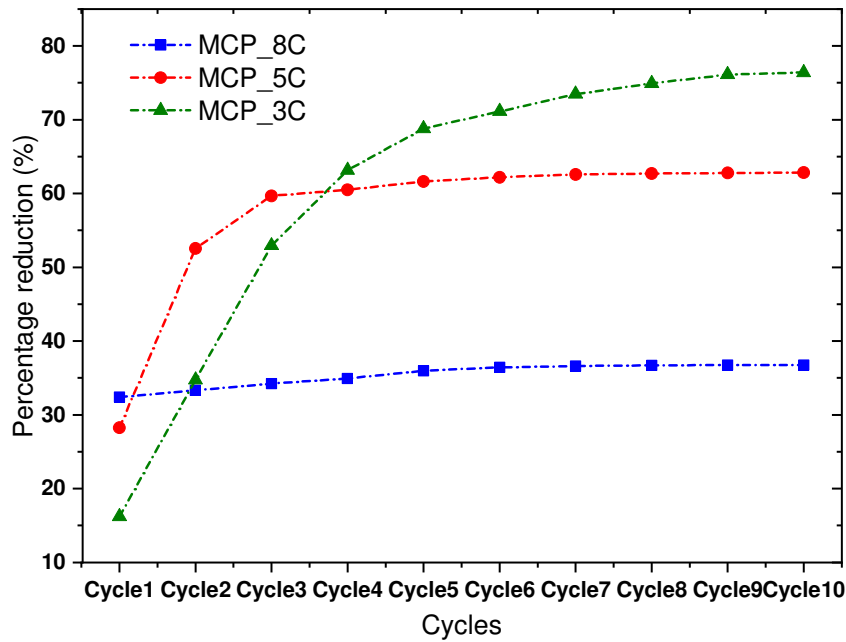
	<i>Reference</i>	<i>RT 8</i>	<i>RT 5</i>	<i>RT 3</i>
Total recovery cooling capacity (kWh)	154.43	99.74	65.54	60.44
Total energy saving (kWh)	--	54.68	88.88	93.98

351

352 [Fig. 17] illustrates the percentage reduction of cooling energy inside the refrigerated
 353 container using different PCM concepts compared to the conventional truck. Thus, the current
 354 concept using RT3 HC1, RT5, and RT8 HC proves to be capable of reducing the cooling
 355 energy required when opening the door by 61%, 57%, and 35%, respectively. Therefore, this
 356 reduction in cooling energy consumption leads to energy savings and reduced pollution from
 357

358 conventional refrigeration units. As a result, the cooling system is improved with a specific
359 cooling temperature, which corresponds to the type of PCM used.

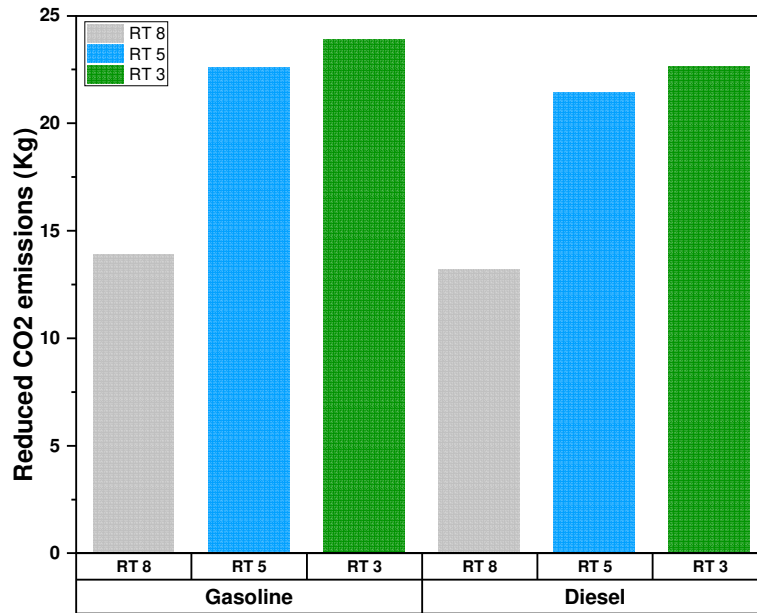
360 Considering all the PCMs investigated, the results indicate that the most efficient thermal
361 behavior was obtained using RT3 HC1 paraffin under the operating conditions presented in
362 this study. This reflects the performance of RT3 HC1, that offers energy savings of up to 61%
363 compared to the conventional system.



364 **Fig. 17** Percentage reduction of cooling energy using different PCM concepts
365

366 4.6. Environmental impact

367 The use of PCM provides a high thermal inertia, leading to a reduction of the heat exchange
368 rate. In fact, the environmental aspect must be taken into account when assessing energy
369 systems. In this context, GHG emissions are calculated according to the energy saved, after
370 using the PCM for conventional cooling units, and the correspondent CO₂ emission factor
371 [48]. The authors considered the emissions factor of the diesel and gasoline medium-duty
372 truck were 0.254 kg CO_{2eq} / kWh and 0.241 kg CO_{2eq} / kWh, respectively, according to the
373 emission factor database for Europe [49]. Therefore, [Fig.18] represents the amount of
374 reduced CO₂ emissions due to the different PCM incorporation. These results demonstrate
375 that a reduction in the energy flow caused by hot air infiltration during all door opening
376 periods significantly reduces pollutant emissions, which offers an advantage for sustainable
377 development in the refrigerated transport sector.



378

379

Fig. 18 Quantities of reduced GHG emissions

380 5. Conclusion

381 Temperature fluctuations during loading/unloading constitute major issues in food
 382 transportation. Therefore, the incorporation of PCMs in refrigerated trucks offers a promising
 383 solution, as it guarantees product quality and preserves perishable goods. For this purpose, a
 384 physical model was carried out to study the energy performance of refrigerated trucks under
 385 two scenarios: with and without PCM.

386 Besides, the PCM has been incorporated in a module containing several baffle-type panels
 387 placed in the truck's roof. This concept represents an original solution to store the cold during
 388 the truck operation and to release it later. Also, three PCMs (RT3 HC1, RT5 and RT8 HC) are
 389 tested and compared to identify the best one that guarantees the acquired temperature range. It
 390 is found that the use of PCM reduces significantly the cooling energy required when opening
 391 the truck door. Air temperature fluctuations inside the refrigerated trucks during periods after
 392 turning off the cooling system are also reduced by using PCM. Thus, the current concept
 393 using RT3 HC1, RT5, and RT8 HC proves to be capable of reducing the cooling energy
 394 required when opening the door by 61%, 57%, and 35%, respectively. As a result, the
 395 integration of PCM inside the refrigerated truck can lead to an increase in both the
 396 refrigeration system life and the energy savings, and a decrease in GHG gases.

397 Finally, to address more complex tasks related to improving the refrigerated truck energy
 398 performance, further developments can be considered as perceptive of this study such as:

- 399
- Simulation of combined phenomena during a trip considering the internal conditions and the surrounding environment that will result in variation of air temperature and relative humidity inside the truck.
- 400
- 401
- 402
- Evaluation of the thermal loads and the filling effect for certain types of perishable goods inside the refrigerated truck during the journey, taking into account the geometric variations of the road.
- 403
- 404
- Optimization study of the proposed storage system design taking into account the number of rods containing the PCM, as well as the spacing between these rods.
- 405
- 406

407

408

409

410

411

412

413

414

415

416

417

418

419

420

421

422

423

424

425 **References:**

- 426 [1] A.R. Shaibani, M.M. Keshtkar, P. Talebizadeh Sardari, Thermo-economic analysis of a
427 cold storage system in full and partial modes with two different scenarios: A case
428 study, *J. Energy Storage*. 24 (2019) 100783. <https://doi.org/10.1016/j.est.2019.100783>.
- 429 [2] M. Kayfeci, A. Keçebaş, E. Gedik, Determination of optimum insulation thickness of
430 external walls with two different methods in cooling applications, *Appl. Therm. Eng.*
431 50 (2013) 217–224. <https://doi.org/10.1016/j.applthermaleng.2012.06.031>.
- 432 [3] S.J. James, C. James, The food cold-chain and climate change, *Food Res. Int.* 43
433 (2010) 1944–1956. <https://doi.org/10.1016/j.foodres.2010.02.001>.
- 434 [4] M.A. Ben Taher, Z. Benseddik, A. Afass, S.Smouh, M. Ahachad, M. Mahdaoui,
435 Energy life cycle cost analysis of various solar water heating systems under Middle
436 East and North Africa region, *Case Stud. Therm. Eng.* (2021) 101262.
437 <https://doi.org/10.1016/j.csite.2021.101262>.
- 438 [5] H.J. Xu, C.Y. Zhao, Thermal performance of cascaded thermal storage with phase-
439 change materials (PCMs). Part II: Unsteady cases, *Int. J. Heat Mass Transf.* 106 (2017)
440 945–957. <https://doi.org/10.1016/j.ijheatmasstransfer.2016.10.066>.
- 441 [6] E. Oró, L. Miró, M.M. Farid, L.F. Cabeza, Thermal analysis of a low temperature
442 storage unit using phase change materials without refrigeration system, *Int. J. Refrig.*
443 35 (2012) 1709–1714. <https://doi.org/10.1016/j.ijrefrig.2012.05.004>.
- 444 [7] N. Kayansayan, E. Alptekin, M.A. Ezan, Analyse thermique du débit d’air à l’intérieur
445 d’un conteneur réfrigéré, *Int. J. Refrig.* 84 (2017) 76–91.
446 <https://doi.org/10.1016/j.ijrefrig.2017.08.008>.
- 447 [8] A. Ashok, M. Brison, Y. LeTallec, Improving cold chain systems: Challenges and
448 solutions, *Vaccine*. 35 (2017) 2217–2223.
449 <https://doi.org/10.1016/j.vaccine.2016.08.045>.
- 450 [9] M.A. Ben Taher, T. Kousksou, H. Makroum, M. Ahachad, M. Mahdaoui, Numerical
451 Study of a Non-isothermal Refrigerated Truck, *Adv. Intell. Syst. Comput.* 1104 AISC
452 (2020) 484–491. https://doi.org/10.1007/978-3-030-36671-1_43.
- 453 [10] H.J. Xu, C.Y. Zhao, Analytical considerations on optimization of cascaded heat
454 transfer process for thermal storage system with principles of thermodynamics, *Renew.*

- 455 Energy. 132 (2019) 826–845. <https://doi.org/10.1016/j.renene.2018.07.135>.
- 456 [11] M. Mahdaoui, S. Hamdaoui, A. Ait Msaad, T. Kousksou, T. El Rhafiki, A. Jamil, M.
457 Ahachad, Building bricks with phase change material (PCM): Thermal performances,
458 Constr. Build. Mater. 269 (2021) 121315.
459 <https://doi.org/10.1016/j.conbuildmat.2020.121315>.
- 460 [12] H. Bagheri-Esfah, H. Safikhani, S. Motahar, Multi-objective optimization of cooling
461 and heating loads in residential buildings integrated with phase change materials using
462 the artificial neural network and genetic algorithm, J. Energy Storage. 32 (2020)
463 101772. <https://doi.org/10.1016/j.est.2020.101772>.
- 464 [13] F. Rouault, D. Bruneau, P. Sebastian, J. Lopez, Multiobjective optimization of an air-
465 phase change material heat exchanger for free cooling in a single-family house, J.
466 Energy Storage. 32 (2020) 101944. <https://doi.org/10.1016/j.est.2020.101944>.
- 467 [14] S. Hamdaoui, M. Mahdaoui, T. Kousksou, Y. El Afou, A. Ait Msaad, A. Arid, A.
468 Ahachad, Thermal behaviour of wallboard incorporating a binary mixture as a phase
469 change material, J. Build. Eng. 25 (2019) 100820.
470 <https://doi.org/10.1016/j.jobe.2019.100820>.
- 471 [15] M.M.A. Khan, R. Saidur, F.A. Al-Sulaiman, A review for phase change materials
472 (PCMs) in solar absorption refrigeration systems, Renew. Sustain. Energy Rev. 76
473 (2017) 105–137. <https://doi.org/10.1016/j.rser.2017.03.070>.
- 474 [16] F.S. Javadi, H.S.C. Metselaar, P. Ganesan, Performance improvement of solar thermal
475 systems integrated with phase change materials (PCM), a review, Sol. Energy. 206
476 (2020) 330–352. <https://doi.org/10.1016/j.solener.2020.05.106>.
- 477 [17] A. Touzo, R. Olives, G. Dejean, D. Pham Minh, M. El Hafi, J.-F. Hoffmann, X. Py,
478 Experimental and numerical analysis of a packed-bed thermal energy storage system
479 designed to recover high temperature waste heat: an industrial scale up, J. Energy
480 Storage. 32 (2020) 101894. <https://doi.org/10.1016/j.est.2020.101894>.
- 481 [18] M.A. BEN TAHER, H. El-Otmany, T. El Rhafiki, T. Kousksou, Y. Zeraouli, Inverse
482 method to describe crystallization of undercooled water in cold storage tank, J. Energy
483 Storage. 36 (2021) 102404. <https://doi.org/10.1016/j.est.2021.102404>.
- 484 [19] H.J. Xu, C.Y. Zhao, Thermal performance of cascaded thermal storage with phase-

- 485 change materials (PCMs). Part I: Steady cases, *Int. J. Heat Mass Transf.* 106 (2017)
486 932–944. <https://doi.org/10.1016/j.ijheatmasstransfer.2016.10.054>.
- 487 [20] H.J. Xu, C.Y. Zhao, Thermal efficiency analysis of the cascaded latent heat/cold
488 storage with multi-stage heat engine model, *Renew. Energy.* 86 (2016) 228–237.
489 <https://doi.org/10.1016/j.renene.2015.08.007>.
- 490 [21] E. Oró, E. de Jong, L.F. Cabeza, Experimental analysis of a car incorporating phase
491 change material, *J. Energy Storage.* 7 (2016) 131–135.
492 <https://doi.org/10.1016/j.est.2016.05.003>.
- 493 [22] J. Du, B. Nie, Y. Zhang, Z. Du, L. Wang, Y. Ding, Cooling performance of a thermal
494 energy storage-based portable box for cold chain applications, *J. Energy Storage.* 28
495 (2020) 101238. <https://doi.org/10.1016/j.est.2020.101238>.
- 496 [23] Y. Zhao, X. Zhang, X. Xu, S. Zhang, Development of composite phase change cold
497 storage material and its application in vaccine cold storage equipment, *J. Energy
498 Storage.* 30 (2020) 101455. <https://doi.org/10.1016/j.est.2020.101455>.
- 499 [24] S. Talukdar, H.M.M. Afroz, M.A. Hossain, M.A. Aziz, M.M. Hossain, Heat transfer
500 enhancement of charging and discharging of phase change materials and size
501 optimization of a latent thermal energy storage system for solar cold storage
502 application, *J. Energy Storage.* 24 (2019) 100797.
503 <https://doi.org/10.1016/j.est.2019.100797>.
- 504 [25] I. Dincer, On thermal energy storage systems and applications in buildings, *Energy
505 Build.* 34 (2002) 377–388. [https://doi.org/10.1016/S0378-7788\(01\)00126-8](https://doi.org/10.1016/S0378-7788(01)00126-8).
- 506 [26] C. Veerakumar, A. Sreekumar, Phase change material based cold thermal energy
507 storage: Materials, techniques and applications – A review, *Int. J. Refrig.* 67 (2016)
508 271–289. <https://doi.org/10.1016/j.ijrefrig.2015.12.005>.
- 509 [27] M. Liu, W. Saman, F. Bruno, Development of a novel refrigeration system for
510 refrigerated trucks incorporating phase change material, *Appl. Energy.* 92 (2012) 336–
511 342. <https://doi.org/10.1016/j.apenergy.2011.10.015>.
- 512 [28] M. Gaedtke, S. Wachter, S. Kunkel, S. Sonnick, M. Rädle, H. Nirschl, M.J. Krause,
513 Numerical study on the application of vacuum insulation panels and a latent heat
514 storage for refrigerated vehicles with a large Eddy lattice Boltzmann method, *Heat*

- 515 Mass Transf. Und Stoffuebertragung. 56 (2020) 1189–1201.
516 <https://doi.org/10.1007/s00231-019-02753-4>.
- 517 [29] H. Tan, Y. Li, H. Tuo, Theoretical and experimental study on a self-refrigerating
518 system for LNG-fueled refrigerated vehicles, *J. Nat. Gas Sci. Eng.* 20 (2014) 192–199.
519 <https://doi.org/10.1016/j.jngse.2014.06.022>.
- 520 [30] H. Tan, Y. Li, H. Tuo, M. Zhou, B. Tian, Experimental study on liquid/solid phase
521 change for cold energy storage of Liquefied Natural Gas (LNG) refrigerated vehicle,
522 *Energy*. 35 (2010) 1927–1935. <https://doi.org/10.1016/j.energy.2010.01.006>.
- 523 [31] M. Ahmed, O. Meade, M.A. Medina, Reducing heat transfer across the insulated walls
524 of refrigerated truck trailers by the application of phase change materials, *Energy*
525 *Convers. Manag.* 51 (2010) 383–392. <https://doi.org/10.1016/j.enconman.2009.09.003>.
- 526 [32] B. Xia, D.-W. Sun, Applications of computational fluid dynamics (cfd) in the food
527 industry: a review, *Comput. Electron. Agric.* 34 (2002) 5–24.
528 [https://doi.org/10.1016/S0168-1699\(01\)00177-6](https://doi.org/10.1016/S0168-1699(01)00177-6).
- 529 [33] E. Oró, L. Miró, M.M. Farid, L.F. Cabeza, Improving thermal performance of freezers
530 using phase change materials, *Int. J. Refrig.* 35 (2012) 984–991.
531 <https://doi.org/10.1016/j.ijrefrig.2012.01.004>.
- 532 [34] A. Tinti, A. Tarzia, A. Passaro, R. Angiuli, Thermographic analysis of polyurethane
533 foams integrated with phase change materials designed for dynamic thermal insulation
534 in refrigerated transport, *Appl. Therm. Eng.* 70 (2014) 201–210.
535 <https://doi.org/10.1016/j.applthermaleng.2014.05.003>.
- 536 [35] A. Mousazade, R. Rafee, M.S. Valipour, Thermal Performance of Cold Panels with
537 Phase Change Materials in a Refrigerated Truck, *Int. J. Refrig.* (2020).
538 <https://doi.org/10.1016/j.ijrefrig.2020.09.003>.
- 539 [36] R. Fioretti, P. Principi, B. Copertaro, A refrigerated container envelope with a PCM
540 (Phase Change Material) layer: Experimental and theoretical investigation in a
541 representative town in Central Italy, *Energy Convers. Manag.* 122 (2016) 131–141.
542 <https://doi.org/10.1016/j.enconman.2016.05.071>.
- 543 [37] A. Rai, J. Sun, S.A. Tassou, Numerical investigation of the protective mechanisms of
544 air curtain in a refrigerated truck during door openings, *Energy Procedia*. 161 (2019)

- 545 216–223. <https://doi.org/10.1016/j.egypro.2019.02.084>.
- 546 [38] P.B.T. Jara, J.J.A. Rivera, C.E.B. Merino, E.V. Silva, G.A. Farfán, Thermal behavior
547 of a refrigerated vehicle: Process simulation, *Int. J. Refrig.* 100 (2019) 124–130.
548 <https://doi.org/10.1016/j.ijrefrig.2018.12.013>.
- 549 [39] E. Oró, A. Gil, L. Miró, G. Peiró, S. Álvarez, L.F. Cabeza, Thermal Energy Storage
550 Implementation Using Phase Change Materials for Solar Cooling and Refrigeration
551 Applications, *Energy Procedia.* 30 (2012) 947–956.
552 <https://doi.org/10.1016/j.egypro.2012.11.107>.
- 553 [40] Rubitherm GmbH, Rubitherm Technologies GmbH, (2019). www.rubitherm.eu
554 (accessed May 2, 2020).
- 555 [41] W.. Jones, B.. Launder, The prediction of laminarization with a two-equation model of
556 turbulence, *Int. J. Heat Mass Transf.* 15 (1972) 301–314. [https://doi.org/10.1016/0017-](https://doi.org/10.1016/0017-9310(72)90076-2)
557 [9310\(72\)90076-2](https://doi.org/10.1016/0017-9310(72)90076-2).
- 558 [42] D.C. Wilcox, Reassessment of the scale-determining equation for advanced turbulence
559 models, *AIAA J.* 26 (1988) 1299–1310. <https://doi.org/10.2514/3.10041>.
- 560 [43] F.R. Menter, Two-equation eddy-viscosity turbulence models for engineering
561 applications, *AIAA J.* 32 (1994) 1598–1605. <https://doi.org/10.2514/3.12149>.
- 562 [44] M. Zeneli, A. Nikolopoulos, S. Karellas, N. Nikolopoulos, Numerical methods for
563 solid-liquid phase-change problems, in: A.B.T.-U.-H.T.T.E.S. Datas Transfer and
564 Conversion (Ed.), *Ultra-High Temp. Therm. Energy Storage, Transf. Convers.*,
565 Elsevier, 2021: pp. 165–199. <https://doi.org/10.1016/B978-0-12-819955-8.00007-7>.
- 566 [45] Y. Khattari, H. El-Otmany, T. El Rhafiki, T. Kousksou, A. Ahmed, E. Ben Ghoulam,
567 Physical models to evaluate the performance of impure phase change material
568 dispersed in building materials, *J. Energy Storage.* 31 (2020) 101661.
569 <https://doi.org/10.1016/j.est.2020.101661>.
- 570 [46] G. Panozzo, G. Cortella, Standards for transport of perishable goods are still adequate?,
571 *Trends Food Sci. Technol.* 19 (2008) 432–440.
572 <https://doi.org/10.1016/j.tifs.2008.03.007>.
- 573 [47] D. Rovňaníková, Comparison of the Temperature Conditions in the Transport of
574 Perishable Foodstuff, *Open Eng.* 7 (2017) 115–120. [29](https://doi.org/10.1515/eng-2017-</p></div><div data-bbox=)

575 0017.

576 [48] E. Oró, L. Miró, M.M. Farid, V. Martin, L.F. Cabeza, Energy management and CO2
577 mitigation using phase change materials (PCM) for thermal energy storage (TES) in
578 cold storage and transport, *Int. J. Refrig.* 42 (2014) 26–35.
579 <https://doi.org/10.1016/j.ijrefrig.2014.03.002>.

580 [49] Ecometrica, Emission Factors, (2021). <https://emissionfactors.com/>.

581